

**Emission patterns of neutral pions in 40A MeV Ta + Au reactions**

K. Piasecki,<sup>1,\*</sup> T. Matulewicz,<sup>1</sup> N. Yahlali,<sup>2</sup> H. Delagrange,<sup>3,4</sup> J. Díaz,<sup>2</sup> D. G. d'Enterria,<sup>3,†</sup> F. Fernández,<sup>5</sup> A. Kugler,<sup>6</sup> H. Löhner,<sup>7</sup> G. Martínez-García,<sup>3,4</sup> R. W. Ostendorf,<sup>7</sup> Y. Schutz,<sup>3,4,‡</sup> P. Tlustý,<sup>6</sup> R. Turrisi,<sup>4,‡</sup> V. Wagner,<sup>6</sup> and H. W. Wilschut<sup>7</sup>  
(TAPS Collaboration)

<sup>1</sup>*Institute of Experimental Physics, University of Warsaw, Hoża 69, PL-00-681 Warsaw, Poland*

<sup>2</sup>*Institut de Física Corpuscular, Universitat de Valencia-CSIC, Dr Moliner 50, E-46100 Burjassot, Spain*

<sup>3</sup>*SUBATECH, (CNRS/IN2P3, Ecole des Mines de Nantes, Université de Nantes), Nantes, France*

<sup>4</sup>*GANIL, IN2P3-CNRS, DSM-CEA, F-14076 Caen Cedex 5, France*

<sup>5</sup>*Grup de Física de les Radiacions, Universitat Autònoma de Barcelona E-08193, Catalonia, Spain*

<sup>6</sup>*Nuclear Physics Institute of the ASCR, CZ-25068 Řež, Czech Republic*

<sup>7</sup>*Kernfysisch Versneller Instituut, NL-9747 AA Groningen, The Netherlands*

(Received 9 September 2009; revised manuscript received 15 April 2010; published 28 May 2010)

Differential cross sections of neutral pions emitted in  $^{181}\text{Ta}+^{197}\text{Au}$  collisions at a beam energy of 39.5A MeV have been measured with the two-arm photon spectrometer (TAPS). The kinetic energy and transverse momentum spectra of neutral pions cannot be properly described in the framework of the thermal model, nor when the reabsorption of pions is accounted for in a phenomenological model. However, high energy and high momentum tails of the pion spectra can be well fitted through thermal distributions with unexpectedly soft temperature parameters below 10 MeV.

DOI: [10.1103/PhysRevC.81.054912](https://doi.org/10.1103/PhysRevC.81.054912)

PACS number(s): 25.70.-z, 25.75.Dw

**I. INTRODUCTION**

Neutral pion emission is a very sensitive probe of the processes taking place in the interaction zone of two nuclei colliding at beam energies below 100A MeV. This energy is well below the free nucleon-nucleon ( $NN$ )  $\pi^0$  threshold of 280 MeV. In consequence, the energy of produced mesons is limited, even with the help of the cooperative effect of Fermi motion. This energy limitation allows the experimental study of the energy spectrum and angular distribution of  $\pi^0$  mesons to a large extent. In addition, the dominant two-photon decay channel of this short-lived meson makes possible the detection of neutral pions also at rest. The number of detected neutral pions, superior to the previous measurement [1,2], allows us to make more definitive conclusions about their spectral properties.

With decreasing beam energy per nucleon, the particle production process increasingly relies on the internal motion of nucleons and their correlations (cooperative effects) as well as on the dynamical evolution of the colliding system. The particles produced in these unfavorable conditions carry important information about the collision process, as they remove a significant fraction of the available energy. Various models have attempted to describe these processes. Fermi motion, which plays a crucial role in subthreshold particle production, is, of course, incorporated in modern transport model calculations (e.g., Ref. [3]). These models include baryonic resonances, which serve as a temporary energy storage enabling the production of mesons. However, while

the gross properties of subthreshold particle production are relatively well explained by these models, the description of spectral properties of neutral pions does not always provide satisfactory results. While for Ar + Al collisions at 95A MeV a rather consistent description of  $\pi^0$  emission was found [4], the yield of neutral pions from Kr + Ni collisions at 60A MeV was strongly underpredicted in the high energy part of the spectrum [5]. Phenomenological models of first-chance nucleon-nucleon collisions have also been used to describe the energy scaling of the cross sections (e.g., Ref. [6]). In another extreme, purely thermal models of particle emission have been applied to describe the interaction zone of two colliding nuclei [7]. Strong reabsorption processes of pions in the nuclear medium have been incorporated into both the transport and thermal models [4,7,8].

The production of neutral pions was studied with the two-arm photon spectrometer (TAPS) [9] for a nearly symmetric heavy system  $^{181}\text{Ta} + ^{197}\text{Au}$  at a beam energy of 39.5A MeV, i.e., at 1/7 of the free  $NN$   $\pi^0$  production threshold energy. Particular attention was paid to removing all effects that could obscure the experimental data for such rarely produced particles. The contribution from cosmic radiation was reduced to below 1% of the final neutral pion sample.

**II. EXPERIMENTAL SETUP**

In the experiment performed at the Grand Accélérateur National d'Ions Lourds (GANIL),  $^{181}\text{Ta}^{57+}$  ions were accelerated to 39.5A MeV beam energy and delivered in bunches with a rate of 9.055 MHz. The nominal beam intensity was 10 enA, ca. 160 ions per pulse. The Ta ions impinged on a 19.3 mg/cm<sup>2</sup> thick  $^{197}\text{Au}$  target. The interaction probability per average beam pulse was about 7%.

\*Krzysztof.Piasecki@fuw.edu.pl

†Present address: CERN, CH-1211 Genève, Switzerland.

‡Present address: INFN-Padova, Via Marzolo 8, IT-35131 Padova, Italy.

Photon pairs originating from  $\pi^0$  decays were detected by the TAPS electromagnetic calorimeter [9], arranged in six blocks, each composed of 64 hexagonal modules in an  $8 \times 8$  honeycomb structure. The configuration of the experimental setup was shown in Fig. 1 of Ref. [10] (in our measurement the inner detectors Dwarf Ball and SSD were removed). The blocks covered a wide range of polar angles (between  $45^\circ$  and  $170^\circ$ ), making up about 20% of the full solid angle. Each module consisted of a 25-cm-long  $\text{BaF}_2$  crystal (corresponding to 12 radiation lengths) of hexagonal cross section with an inscribed radius of 2.95 cm. A charged particle veto detector (CPV) made of plastic scintillator NE102A was mounted in front of each module. Events with neutral pion candidates were selected by a trigger, requiring activation of at least two modules by neutral particles, in different TAPS blocks. An activation was defined by depositing energy of about 12 MeV, a value not affecting the measurement of energy distribution of photons originating from neutral pion decays.

### III. DATA ANALYSIS

A single TAPS module measures the time, energy, and electric charge state (neutral or charged) of the incoming particle. The scintillation light response of  $\text{BaF}_2$  has two components, whose relative intensity differs for electrons (and photons) compared to heavily-ionizing particles like protons and deuterons [11]. This feature, combined with the time of flight (TOF) information and the charge veto signal, delivers nearly unambiguous identification of a photon [12]. This particle, traversing the  $\text{BaF}_2$  module, induces an electromagnetic cascade which usually spreads into adjacent modules, creating a cluster of active modules. The properties of a particle were reconstructed from a cluster using the ROSEBUD [13] analysis package. If a particle hits the border of a TAPS block, part of the induced cascade can escape the detector. Such a cluster was rejected by requiring that the maximum energy deposition cannot be in a border module (cf. [12]). Cosmic radiation was filtered out by a series of dedicated algorithms [14–16]. They make use of differences between photon and cosmic-ray induced clusters in the topology-based signatures: the multiplicity of active modules in a cluster, the linearity of its shape, and the intrinsic dispersion of the energy distribution in modules calculated with respect to the most energetic one. The invariant mass distribution of  $\gamma\gamma$  pairs obtained is shown in the upper panel of Fig. 1 and exhibits a prominent  $\pi^0$  peak. The invariant mass resolution (full width at half maximum, FWHM) of this peak is 11%, in agreement with Monte Carlo simulations [12]. The observed shoulder for masses below  $m_{\pi^0}$  is due to a partial escape of the electromagnetic cascade from a TAPS block [17]. The high signal-to-background ratio  $S/B = 18$  allows selection of the  $\pi^0$  candidates on an event-by-event basis.

A kinematical fit [18] was applied to each event to improve the quality of the reconstruction of neutral pion momentum from the momenta of the photons in a pair associated with the meson decay, taking advantage of the known neutral pion mass. The parameters of this method, the invariant mass threshold  $m_{\gamma\gamma}^{\min}$  and the maximum chi-square of the event reconstruction

$\chi_{\max}^2$ , were adjusted such that the distributions of pulls of the three-momentum components were in the best agreement with the normal distribution. The best fit parameters were found to be  $m_{\gamma\gamma}^{\min} = 105 \text{ MeV}/c^2$  and  $\chi_{\max}^2 = 20$ . The influence of their variation on the results presented in this paper was added to the corresponding systematic errors. The bremsstrahlung photon pairs from the Ta + Au collision zone were automatically rejected by these conditions (mainly by the  $m_{\gamma\gamma}^{\min}$  cut). A total of 528 photon pairs satisfied all the above-mentioned filters and were assigned to  $\pi^0$  decays. The contribution of cosmic radiation was found to be on the level of below one pair.

The phase space population of measured neutral pions is shown in the bottom panel of Fig. 1 in the plane of rapidity and transverse momentum, where the midrapidity in the AA frame ( $y_{\text{c.m.}}^{AA}$ ) is indicated by an arrow. The dashed curve shows the average momentum of  $\pi^0$  emitted from a source obeying the Boltzmann distribution [Eq. (1)] with a temperature of 15 MeV. This value is typical for the inverse slopes of momentum distributions of neutral pions at beam energies around 40A MeV [1,19,20]. The expected phase space distribution of neutral pions is well covered by the experimental data. To account for the detection efficiency, neutral pions were sampled from a Boltzmann distribution without collective radial flow of a particle [21]

$$\frac{d^2\sigma}{dp_T dy} \sim p_T E \exp(-E/T), \quad (1)$$

where  $T$  is the temperature of the source,  $E = m_T c^2 \cosh(y)$  is used, and  $m_T$  is the transverse mass  $m_T c^2 = \sqrt{(p_T c)^2 + (m_T c^2)^2}$  [22]. The response of the TAPS apparatus was simulated using the GEANT3-based [23] KANE code [24]. The source temperatures were varied between 6 and 24 MeV, i.e., a range of inverse slopes of transverse momentum

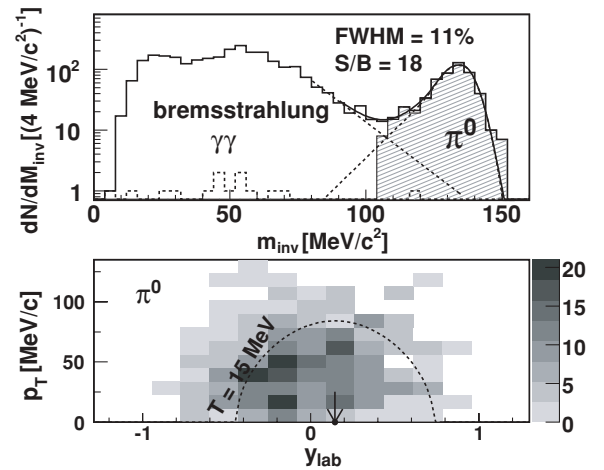


FIG. 1. Top: invariant mass distribution of photon pairs shown with fit of an asymmetric Gaussian function to the  $\pi^0$  peak and an exponential background. Hatched histogram: the  $\pi^0$  candidates after the kinematical fit selection; dashed histogram: contamination from cosmic radiation. Bottom: Phase space distribution of the reconstructed  $\pi^0$  in the  $p_T$  vs  $y_{\text{lab}}$  plane; dashed curve for the average momentum of the  $\pi^0$  obtained from a Boltzmann distribution characterized by  $T = 15 \text{ MeV}$ ; the arrow indicates the  $y_{\text{c.m.}}^{AA}$  (see text).

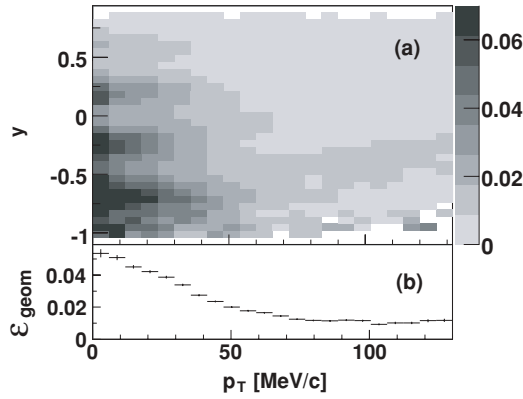


FIG. 2. Top: efficiency of  $\pi^0$  mesons as a function of rapidity and transverse momentum, obtained with the KANE code [24]. Bottom: estimation of geometric component of efficiency, simulated in frame of the PLUTO code [28]. See text for details.

distributions found to be characteristic for beam energies between 25A and 95A MeV [1,19,20,25–27]. The efficiency  $\varepsilon$  of neutral pions was investigated as a function of their rapidity and transverse momentum (see the upper panel of Fig. 2). In the region of  $p_T \lesssim 60$  MeV/c the shape of  $\varepsilon$  changes rapidly. Oscillations in rapidity stem from the geometric configuration of the TAPS blocks. To verify that the sharp drop of efficiency at lower transverse momenta is also due to the geometric setup of TAPS, a thermal source of  $\pi^0$  mesons was generated within the PLUTO [28] code, and boosted according to the  $NN$  frame in the colliding system analyzed. An efficiency  $\varepsilon_{\text{geom}}$  was constructed by selecting events in which both photons from a  $\pi^0$  decay were emitted toward the TAPS blocks. The profile of  $\varepsilon_{\text{geom}}$  as a function of  $p_T$ , shown in the lower panel of Fig. 2, demonstrates that the TAPS geometry is the driving cause of the drop observed in the upper panel of this figure. It also provides a cross-check of the GEANT-based analysis. In the regions of phase space around the limits of observed data, some dependency of the efficiency on  $T$  was found. The existence of this dependency in conjunction with the profile of measured  $p_T$  spectrum (see Fig. 3) is the reason behind using as an input to the KANE efficiency calculation a thermal distribution with a broad range of values of  $T$  parameter, rather than a homogenous spectrum in  $p_T$ - $y$  phase space. Variations of parameters extracted in the present analysis due to the uncertainty of the efficiency map were added to the relevant systematic errors. Because the efficiency changes quite sharply in some regions of  $p_T$  and  $y$ , in order to obtain the weight for every reconstructed neutral pion,  $\varepsilon$  was linearly interpolated between neighboring bins.

The overall  $\pi^0$  acceptance of the apparatus and the applied analysis methods was found to be 0.36%.

#### IV. RESULTS

In the previous measurement of Ta+Au collisions at 39.5A MeV, performed by the TAPS Collaboration, about 100  $\pi^0$  mesons were reconstructed [1,2]. The neutral pion cross section was found to be  $\sigma_{\pi^0} = 2.2 \pm 0.3 \mu\text{b}$ , and the

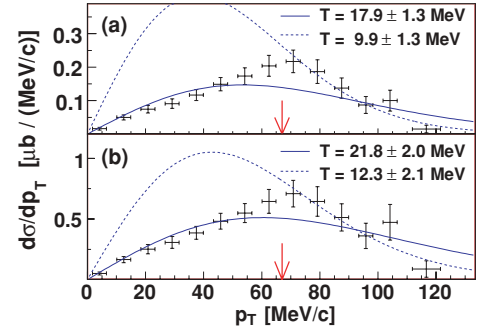


FIG. 3. (Color online) Transverse momentum distribution of neutral pions emitted from Ta+Au collisions at a beam energy of 39.5A MeV, for a  $\Delta y = \pm 0.45$  window around  $y_{\text{c.m.}}^{AA}$ , without (a) and including (b) the model of absorption in nuclear matter (see text). Thermal fits to the whole spectrum (solid lines) and to the high  $p_T$  range (dotted lines) are shown. Arrows indicate the lower bound of the fit to a high  $p_T$  tail of the spectrum.

transverse momentum spectrum was described by a Boltzmann function characterized by a temperature of  $16 \pm 4$  MeV. The cross section for bremsstrahlung photons of energies above 30 MeV,  $\sigma_\gamma = 6.9 \pm 0.7$  mb, was also obtained, thus the ratio of  $\sigma_{\pi^0}/\sigma_\gamma$  was found to be  $(3.2 \pm 0.5) \times 10^{-4}$ .

The analysis presented here is based on a number of identified pions five times larger than the previous measurement. Therefore, we are now able to study the properties of produced pions in more detail. As a cross-check with the previous measurement, the  $\sigma_{\pi^0}/\sigma_\gamma$  ratio was obtained according to the following formula:

$$\frac{\sigma_{\pi^0}}{\sigma_\gamma} = \frac{\sum_{i=1}^{N_\pi} (1/\varepsilon_i^\pi)}{\sum_{i=1}^{N_\gamma} (1/\varepsilon_i^\gamma)}, \quad (2)$$

where  $\varepsilon^{\pi/\gamma}$  are the detection efficiencies of neutral pions and photons, and the summation runs over  $N_{\pi/\gamma}$  accepted particles. The relevant efficiency maps were simulated using the KANE code. The ratio obtained is found to be  $(4.5 \pm 0.4) \times 10^{-4}$ , in  $2\sigma$  agreement with the value found in the previous measurement. For an absolute normalization of the neutral pion distributions presented here, the above-mentioned cross section of  $2.2 \pm 0.3 \mu\text{b}$  from Refs. [1,2] was used.

For a narrow rapidity range  $\Delta y$  around  $y_{\text{c.m.}}^{AA}$ , the Boltzmann distribution expressed by Eq. (1) can be approximated by

$$\frac{d\sigma}{dp_T} \sim p_T m_T \exp\left(-\frac{m_T c^2 \langle \cosh(y) \rangle_{\Delta y}}{T}\right). \quad (3)$$

To fit this function to the experimental data, pions from the  $\Delta y = \pm 0.45$  range were selected. This choice of rapidity range is a balance between the requirement of reasonable statistics and the reliability of the approximation assumed in Eq. (3). Variations of the results presented below due to a choice of  $\Delta y$  were added to the systematic errors. The fit gives an inverse slope of  $17.9 \pm 1.3_{-1.3}^{+0.7}$  MeV [see solid curve in Fig. 3(a) and Table I]. However, a  $\chi^2/\nu$  is found to be 2.5, and the autocorrelations in the residuals of neighboring bins can be observed. The same discrepancy is also observed for the kinetic energy distribution, shown in Fig. 5 and discussed below. The fit of Eq. (3) to the high  $p_T$  part ( $p_T > 67$  MeV/c)

TABLE I. Summary of inverse slopes and polar anisotropy parameters. Also, shown are the estimates of the primordial values of these parameters, calculated within the  $\pi^0$  absorption model described in the text. For the contributions to the systematic errors, see text. The  $p_T$  values are in units of MeV/ $c$ ; the  $T$  values are in MeV. The global fits ( $p_T > 0$ ,  $E_{\text{kin}} > 0$ ) could not describe the spectra well.

Observable	Measured spectrum		Primordial spectrum	
	$p_T > 0$	$p_T > 67$	$p_T > 0$	$p_T > 67$
$T$ from $p_T$ for $ y - y_{\text{c.m.}}^{AA}  < 0.45$	$17.9 \pm 1.3^{+0.7}_{-1.3}$	$9.9 \pm 1.4^{+1.0}_{-0.8}$	$21.8 \pm 2.0$	$12.3 \pm 2.1^{+1.8}_{-1.1}$
$T$ from $E_{\text{kin}}$ for $E_{\text{kin}} > 37$ MeV	$8.7 \pm 1.6^{+0.1}_{-1.3}$		$10.8 \pm 2.2^{+0.2}_{-1.7}$	
$A_2$	$0.31 \pm 0.09^{+0.05}_{-0.02}$		$0.09 \pm 0.09^{+0.03}_{-0.02}$	

delivers an inverse slope parameter of  $T = 9.9 \pm 1.4^{+1.0}_{-0.8}$  MeV, a value considerably lower than the one resulting from the fit in a full  $p_T$  range. However, in this case, the low momentum part of the experimental spectrum is strongly overpredicted by the extrapolation of the fit. This depletion correlates with the decline of efficiency with  $p_T$ , as shown in the upper panel of Fig. 3. However, as reported in Sec. III, an additional simulation verified that the positioning of TAPS blocks was solely responsible for the mentioned drop of efficiency. The findings reported above strongly suggest that the distribution of transverse momentum of neutral pions cannot be fitted globally with the Boltzmann's thermal function. As shown in Table II, this trend has been observed in a range of systems investigated by the TAPS Collaboration at beam energies below 100A MeV [1,19,20,25–27]. The  $p_T$  spectra of neutral pions from other experiments were taken as they were published and fitted both to the full range and with a common lower bound of 60 MeV/ $c$  with the function

$$f(p_T) \sim p_T m_T \exp(-m_T/T). \quad (4)$$

In spite of somewhat different ranges of rapidities accessible to those experiments, in all reported cases the slope obtained

globally was larger than the one fitted to the high  $p_T$  tail of distribution. Therefore, as for the current data, extrapolations of Boltzmann functions fitted to the high  $p_T$  tails overpredicted the measured pion yield at lower transverse momenta. In the measurements performed in the 1980s at 25A and 35A MeV [29,30], no depletion of yield was found. However, those experiments were performed with lead-glass spectrometers, which allowed an invariant mass resolution of only 40%. Also, the experimental setup used in those measurements did not allow the application of advanced procedures for the rejection of cosmic-ray background, which are employed in the analysis presented in our paper.

To estimate the effect of the shadowing of pions by nuclear matter, a simple geometrical model [32,33] was applied. It assumes  $\pi^0$  production from a random point inside a static collision zone defined by the maximum overlap of two spheres at a random impact parameter. Mesons are produced in a thermalized source of temperature  $T_{\text{model}} = 12$  MeV and emitted with an angular distribution:

$$f(\vartheta) = 1 + A_2 P_2(\cos \vartheta), \quad (5)$$

TABLE II. Systematics of inverse slopes obtained by fitting Eq. (4) to the transverse momentum distributions of neutral pions at beam energies below 100A MeV from recent experiments. Global fits ( $p_T > 0$  MeV/ $c$ ) and high  $p_T$  ( $> 60$  MeV/ $c$ ) are shown. When the authors used different functions or when the lower fit bounds for fitting the tail were different than 60 MeV/ $c$ , the data were extracted and refitted.

System	$T_{\text{beam}}$ (A MeV)	$T$ ( $p_T > 0$ ) (MeV)	$T$ ( $p_T > 60$ ) (MeV)	Ref.
Ar + Au	25	$13.3 \pm 2.5$	$6.4 \pm 1.9$	[26], prelim.
Ar + Au	35	$13.0 \pm 0.9$	$11.6 \pm 0.9$	[26], prelim.
Ta + Au	39.5	$17.4 \pm 1.3^{+0.7}_{-1.3}$	$11.0 \pm 1.2^{+1.0}_{-0.8}$	This work
Xe + Au	44	$14.6 \pm 1.0$	$12.7 \pm 1.0$	[19]
Kr + Ni	60	$17.0 \pm 0.5$	$15.8 \pm 0.2$	[1]
Ar + C	60	$16.2 \pm 0.7$	$13.3 \pm 1.0$	[25,31]
Ar + Ni	60	$16.6 \pm 0.6$	$11.9 \pm 0.3$	[25,31]
Ar + Ag	60	$18.3 \pm 2.8$	$16.3 \pm 2.7$	[25,31]
Ar + Au	60	$17.2 \pm 0.8$	$12.7 \pm 0.7$	[25,31]
Ar + C	95	$16.1 \pm 0.2$	$14.2 \pm 0.1$	[25,31]
Ar + Al	95	$18.4 \pm 0.1$	$16.4 \pm 0.1$	[25,31]
Ar + Ag	95	$16.8 \pm 0.2$	$14.1 \pm 0.2$	[25,31]
Ar + Au	95	$15.2 \pm 0.2$	$13.6 \pm 0.2$	[25,31]

where  $P_2$  is the second-order Legendre polynomial and  $A_2 = 0.05$  is the anisotropy parameter.<sup>1</sup> This model uses the momentum-dependent mean free path of a neutral pion [34]. However, it must be noted that neither pion scattering nor the dynamics of the collision is included in this model.

The primordial  $p_T$  distribution estimated by this model is shown in Fig. 3(b). A fit of Eq. (3) performed in the whole range of transverse momenta delivers the inverse slope of  $21.8 \pm 2.0$  MeV and a  $\chi^2/\nu = 1.6$ . This is an improvement compared to  $\chi^2/\nu = 2.5$  for the measured data, so an application of this model brings the distribution somewhat closer to the thermal shape. However, autocorrelations in the residuals of neighboring bins still persist. Fitting the high  $p_T$  tail with a Boltzmann distribution gives a considerably lower inverse slope of  $T = 12.3 \pm 2.1_{-1.1}^{+1.8}$  MeV. However, the fitted function still strongly overestimates the measured yield at lower  $p_T$  values. In the scenario of thermal equilibrium established during the collision, and the system cooling gradually, neutral pions of high  $p_T$  or kinetic energies should be rather characterized by highest temperatures. However, this approach is in contradiction with the findings presented above. The mismatches demonstrated above suggest that neutral pions produced and emitted from the collision zone may not be thermally equilibrated, even if the absorption of neutral pions is accounted for in the frame of the above-mentioned model.

The experimental polar angle distribution of neutral pions in the  $NN$  frame (see Fig. 4) exhibits an anisotropy with less preference for emission in sideward directions. The lack of strong asymmetry between forward and backward directions can be explained by the near symmetry of the colliding system. The pronounced sideward absorption can be qualitatively explained by the longer path of a pion in the colliding nuclear matter due to mutual shadowing by the heavy collision partners. The fit of Eq. (5) to the experimental data yields an anisotropy parameter  $A_2 = 0.31 \pm$

<sup>1</sup>50% variations of  $T_{\text{model}}$  have negligible influence on the obtained corrections. Variations due to changes of  $A_2$  within a  $(-0.5, 0.5)$  interval are small and were included in the systematic errors.

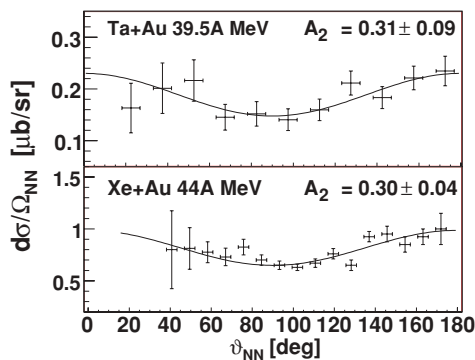


FIG. 4. (Color online) Experimental angular distribution of neutral pions emitted from Ta+Au at 39.5A MeV shown in the  $NN$  frame, compared to Xe+Au at 44A MeV [19]. Curves represent the best fits of the second-order Legendre polynomial (see text).

$0.09_{-0.02}^{+0.05}$ . In an attempt to reconstruct the primordial polar angle distribution of neutral pions, the above-mentioned  $\pi^0$  absorption model was used. To parametrize the primordial spectrum, a dipolar distribution of the form of Eq. (5) was assumed, with an anisotropy parameter  $A_2^{\text{prim}}$ . The angular spectrum of pions which traversed the hadronic matter was compared to the spectrum observed by TAPS. The best fit to the experimental data was obtained for  $A_2^{\text{prim}} = 0.09 \pm 0.09_{-0.02}^{+0.03}$ , which exhibits a near-isotropic emission pattern. Despite the meager experimental knowledge of  $A_2^{\text{prim}}$  values for collisions of symmetric systems at comparable beam energies, an average anisotropy parameter  $A_2^{\text{prim}} = 0.32 \pm 0.05$  for the primordial distribution of all hitherto investigated systems was found [25,33]. This value is quite higher than the one obtained for Ta + Au. However, several values are also beyond the range of the global average quoted above. A fit of Eq. (5) to the angular distribution of neutral pions emitted from  $^{129}\text{Xe} + ^{197}\text{Au}$  collisions at 44A MeV [19] (see bottom panel of Fig. 4) provides an anisotropy parameter of  $A_2 = 0.30 \pm 0.04$ . An estimation of this parameter for the primordial pions done in the framework of the above-mentioned  $\pi^0$  absorption model gives  $A_2^{\text{prim}} = 0.10 \pm 0.04$ . Both values are in very good agreement with results for Ta + Au collisions obtained in this work.

The kinetic energy distribution in the  $NN$  frame has also been investigated. Global fitting by a Maxwellian distribution of the form  $\sim pE \exp(-E/T)$  [see Fig. 5(a)] results qualitatively in the same picture as in the case of the  $p_T$  spectrum: high value of  $\chi^2/\nu = 4.5$  and autocorrelations in the residuals of neighboring bins. A fit of the same function to the high energy tail ( $E_{\text{kin}} > 37$  MeV) gives an inverse slope of  $T = 8.7 \pm 1.6_{-1.3}^{+0.1}$  MeV. Similar to the case of the  $p_T$  distribution, the application of the above-mentioned  $\pi^0$  absorption model results in a slightly increased inverse slope of the high energy tail of the estimated primordial spectrum,  $T = 10.8 \pm 2.2_{-1.7}^{+0.2}$  MeV, and the depletion of the yield in the low  $E_{\text{kin}}$  part of the spectrum cannot be removed [see Fig. 5(b)].

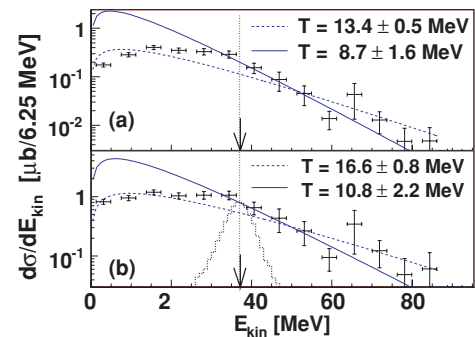


FIG. 5. (Color online) Kinetic energy spectrum of neutral pions, without (a) and including (b) the correction based on the  $\pi^0$  absorption model (see text). Curves represent fits of Maxwellian distribution to the whole spectrum (solid lines) and to the high  $E_{\text{kin}}$  part (dotted lines; vertical lines mark the lower fit bounds). Arrows indicate the kinematical limit for the  $NN \rightarrow NN\pi^0$  reaction including Fermi motion. The TAPS response function for pions emitted with this limiting energy is shown by the dashed lines.

The constructive superposition of the beam momentum and two Fermi momenta of nucleons ( $p_F = 270$  MeV/ $c$ ) from the colliding nuclei enables the production of pions up to kinetic energy of  $E_{\max}^{NN} = 37$  MeV. However, the measured kinetic energy spectrum of neutral pions is spread far beyond this value. The experimental smearing of this upper energy limit, simulated using the KANE code [24], and shown in Fig. 5, cannot explain the extent of the high  $E_{\text{kin}}$  shoulder. One possible hypothesis leading to an explanation of this effect could be the production of pions in channels different from the process  $NN \rightarrow NN\pi^0$ , like the multi-step process (i)  $NN \rightarrow N\Delta$  and  $\Delta N \rightarrow NN\pi^0$  or the cooperative one (ii)  $NNN \rightarrow NNN\pi^0$ . To estimate the kinetic energy limit for each of these processes, which would also take into account the momentum conservation of the reaction products involved, the collisions studied were simulated with the help of the PLUTO code [28]. A kinetic energy of 39.5A MeV was assigned to a “beam nucleon.” The Fermi motion of nucleons was included. In the second step of channel (i) all the available energy was assumed to be transferred to the  $\Delta(1232)$  resonance mass, an assumption justified by the rise of the  $\Delta$  production probability with a resonance mass in the region well below  $\langle m_\Delta \rangle$ . The  $\Delta$  resonance interacted with another nucleon of Fermi gas, originating randomly from the target or beam nuclei. We found that the kinetic energy limits amount to around 75 MeV for both investigated channels. This may be a hint that the investigated channels could play a role in explaining the observed presence of neutral mesons above the  $E_{\max}^{NN}$  limit. On the other hand, calculations within the framework of the Dubna cascade model, assuming  $\pi^0$  production in  $NN$  collisions, and employing inelastic  $\pi N$  scattering [5], systematically underestimated the measured yield in the high energy tail of the spectrum. More systematic investigations of possible

dynamical processes are needed to explain the experimental findings.

## V. CONCLUSIONS

Neutral pions produced in the Ta + Au collision zone at 39.5A MeV were measured using the TAPS electromagnetic calorimeter. Their transverse momentum distribution selected around midrapidity and kinetic energy spectrum deviate from a thermal shape. These deviations cannot be removed by the application of a phenomenological model of  $\pi^0$  absorption in nuclear matter. The kinetic energy spectrum reaches far higher values than the limit for the  $NN \rightarrow NN\pi^0$  channel, including constructive boost of Fermi motion. It is suggested that multistep or cooperative processes could be possible sources of the neutral pion production. Nonetheless, the tails of the  $p_T$  and  $E_{\text{kin}}$  spectra were in agreement with Boltzmann distributions, yielding inverse slope parameters of  $T = 9.9 \pm 1.4^{+1.0}_{-0.8}$  MeV and  $T = 8.7 \pm 1.6^{+0.1}_{-1.3}$  MeV, respectively. The polar angle distribution of the measured pions reveals a dipolar anisotropy characterized by  $A_2 = 0.31 \pm 0.09^{+0.05}_{-0.02}$ . However, the estimated asymmetry of the primordial angular distribution, calculated within the  $\pi^0$  absorption model, turned out to be almost isotropic ( $A_2^{\text{prim}} = 0.09 \pm 0.09^{+0.03}_{-0.02}$ ).

## ACKNOWLEDGMENTS

We thank the GANIL accelerator staff for delivering a high quality beam. This research was supported in part by the Polish State Committee for Scientific Research (KBN) under Grant No. 2P03B 102 25, and by the Spanish Ministerio de Educación y Ciencia under Contract No. FPA2006-12120-C03-02.

- 
- [1] Y. Schutz *et al.*, *Nucl. Phys. A* **622**, 404 (1997).
  - [2] F. M. Marques Moreno, Ph.D. thesis, University of Valence, 1994, GANIL T 94 05 (unpublished).
  - [3] W. Cassing, V. Metag, U. Mosel, and K. Niita, *Phys. Rep.* **188**, 363 (1990).
  - [4] A. Badalà *et al.*, *Phys. Rev. C* **48**, 2350 (1993).
  - [5] K. Gudima *et al.*, *Phys. Rev. Lett.* **76**, 2412 (1996).
  - [6] V. Metag, *Prog. Part. Nucl. Phys.* **30**, 75 (1993).
  - [7] M. D. Zubkov and A. V. Pozdnyakov, *Nucl. Phys. A* **537**, 692 (1992).
  - [8] A. Bonasera, G. Russo, and H. H. Wolter, *Phys. Lett. B* **246**, 337 (1990).
  - [9] H. Ströher, *Nucl. Phys. News* **6**, 7 (1996).
  - [10] R. Ortega *et al.*, *Eur. Phys. J. A* **28**, 161 (2006).
  - [11] R. Novotny, *Nucl. Phys. B: Proc. Suppl.* **61**, 137 (1998).
  - [12] F. M. Marqués, F. Lefèvre, G. Martínez, T. Matulewicz, R. W. Ostendorf, and Y. Schutz, *Nucl. Instrum. Methods A* **365**, 392 (1995).
  - [13] [[www-subatech.in2p3.fr/~photons/taps/rosebud/](http://www-subatech.in2p3.fr/~photons/taps/rosebud/)].
  - [14] K. Piasecki, Ph.D. thesis, University of Warsaw, 2005.
  - [15] T. Matulewicz, P. Lautridou, F. Lefèvre, M. Marqués, G. Martínez, R. Ostendorf, and Y. Schutz, in *Proceedings from the 2nd TAPS Workshop, Guardamar, 1993* (unpublished).
  - [16] G. Martínez, L. Aphecetche, Y. Charbonnier, H. Delagrange, T. Matulewicz, and Y. Schutz, *Nucl. Instrum. Methods A* **391**, 435 (1997).
  - [17] T. Matulewicz *et al.*, *Nucl. Instrum. Methods A* **289**, 194 (1990).
  - [18] K. Korzecka and T. Matulewicz, *Nucl. Instrum. Methods A* **453**, 606 (2000).
  - [19] R. S. Mayer *et al.*, *Phys. Rev. Lett.* **70**, 904 (1993).
  - [20] K. Piasecki, K. Tyminska, and T. Matulewicz, *Acta Phys. Pol. B* **33**, 973 (2002).
  - [21] P. J. Siemens and J. O. Rasmussen, *Phys. Rev. Lett.* **42**, 880 (1979).
  - [22] W.-M. Yao *et al.*, *J. Phys. G* **33**, 1 (2006).
  - [23] [[wwwasdoc.web.cern.ch/wwwasdoc/geant\\_html3/geantall.html](http://wwwasdoc.web.cern.ch/wwwasdoc/geant_html3/geantall.html)].
  - [24] [[www-subatech.in2p3.fr/~photons/taps/kane](http://www-subatech.in2p3.fr/~photons/taps/kane)].
  - [25] K. Tyminska, Ph.D. thesis, University of Warsaw, 2005.
  - [26] N. Yahlali *et al.*, *Nucl. Phys. A* **749**, 190 (2005).
  - [27] K. Tyminska, T. Matulewicz, and K. Piasecki, *Acta Phys. Pol. B* **37**, 161 (2006).
  - [28] I. Frohlich *et al.*, [arXiv:0708.2382](https://arxiv.org/abs/0708.2382) [nucl-ex].
  - [29] J. Stachel *et al.*, *Phys. Rev. C* **33**, 1420 (1986).
  - [30] G. R. Young, F. E. Obenshain, F. Plasil, P. Braun-Munzinger, R. Freifelder, P. Paul, and J. Stachel, *Phys. Rev. C* **33**, 742 (1986).

- [31] K. Tymińska (private communication); preliminary results for  $\pi^0$  measured at 60A MeV were presented in Ref. [20].
- [32] R. Holzmann *et al.*, [Phys. Lett. B](#) **366**, 63 (1996).
- [33] K. Tymińska, T. Matulewicz, and K. Piasecki, [Acta Phys. Pol. B](#) **33**, 981 (2002).
- [34] R. A. Mehrem, H. M. A. Radi, and J. O. Rasmussen, [Phys. Rev. C](#) **30**, 301 (1984).